

# The Choice of the Main Power Components in Electric Traction Converters

Lavinus Sorin Goreci\*, Mihaela Popescu\*\* and Ion Tilă\*

\* S.C. INDA SRL, Research&Development Department, Craiova, România, [lavinus.goreci@inda.ro](mailto:lavinus.goreci@inda.ro), [tila.ion@inda.ro](mailto:tila.ion@inda.ro)  
University of Craiova, Faculty of Electrical Engineering, Craiova, Romania, [mpopescu@em.ucv.ro](mailto:mpopescu@em.ucv.ro)

DOI: 10.52846/AUCEE.2021.1.05

**Abstract** – The choice of the power components of the electric traction converters for autonomous vehicles is a very important aspect in their design. The attention in this paper is first focused on the choice of the DC link capacitor, followed by choice of the IGBT modules, their testing and cooling. Then, the choice of power cables is approached. A dedicated test bench for electric traction converters for autonomous vehicles was designed and achieved. In defining the parameters of the test bench, various possible applications on battery-powered vehicles were taken into account, but also their performances, technical characteristics and functional characteristics. An important share belongs to the integrated propulsion/charging system of the Li-Ion battery developed by the company SC INDA SRL. It is already used in automotive on full-electric trucks and in the battery-powered electric locomotives.

**Cuvinte cheie:** vehicul autonom, IGBT, condensator de curent continuu, inverter, radiator, răcire, MELCOSIM.

**Keywords:** autonomous vehicle, IGBT, DC link capacitor, inverter, heat sink, cooling, MELCOSIM.

## I. INTRODUCTION

Currently, high voltage and current IGBTs are state-of-the-art power electronics modules for the electric traction converters for autonomous vehicles [1-5]. The IGBT itself is part of a complex power kit which includes besides the transistor, input capacitors, laminated bus bars, the cooling system, gate drives etc. For reliable operation the choice of these components is not an easy task considering the technical characteristics of the traction systems.

The best features of a high power IGBT module are closely related to a reliable and high quality protection for IGBT drivers [1]. The attention in [2] is directed towards the connection between a reliable operation of IGBT modules and three important requirements that they have to fulfill: high junction temperature limit, large safe operating area, high current capacity. Methods for obtaining IGBT switching frequency limits are discussed in [3]. A comparison between switching characteristics and losses of IGBT modules for traction applications is studied experimentally in [4]. Reference [5] describes the equations for the power losses evaluation and passive elements design.

The test bench described below includes the designed inverters in the final purpose of a subsidiary contract to the PACETSINEFEN project within the Competitiveness Operational Program, European Regional Development Fund [6]. A block diagram is presented in Fig. 1, where:

TR – three-phase transformer with control sockets;  
R – three-phase rectifier;  
INV1, INV2 – three-phase inverters;  
Ct – DC link capacitor;

CF – braking chopper;  
RF – braking resistor;  
MAS1 – asynchronous machine (motor mode);  
MAS2 – asynchronous machine (generator mode);  
TU<sub>i</sub> – voltage transducers;  
TC<sub>i</sub> – current transducers;  
TG1, TG2 – speed transducers;  
TCP – torque transducers;  
UCR – electronic control unit.

The testbench consists of two asynchronous machines (MAS1, MAS2) mechanically coupled, the first one operating in motor mode and the second in generator mode. The rated power of each machine is 155 kW and in short-term overload mode they allow 390 kW. This ensures a wide range of tests with power up to 400 kW. The two asynchronous machines are supplied by two inverters INV1 and INV2 with PWM (pulse width modulation) control and variable frequency according to the operating modes. The two inverters have a classic structure and have a common DC link. The energy consumed by MAS1 in the motor mode is taken from MAS2 which operates in generator mode and motor – generator system losses are taken from the power supply

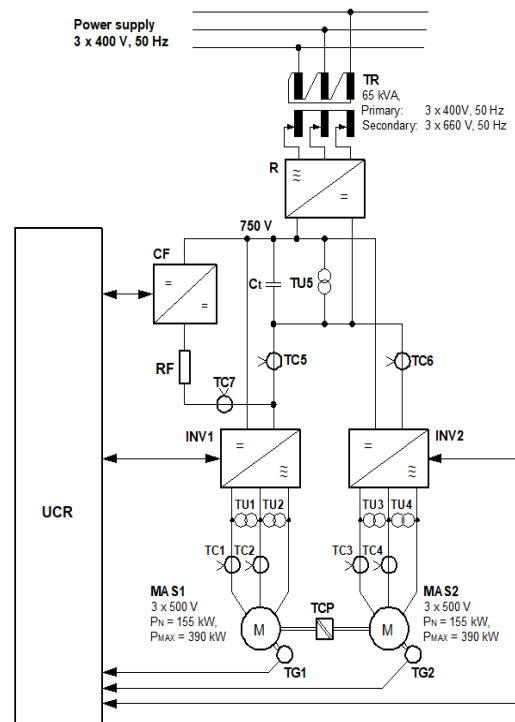


Fig. 1 The block diagram of the test bench.

(3x400 V, 50 Hz) through the transformer TR and rectifier R. For the situation of dynamic regime in the intermediate

circuit, an RF braking resistor is provided, the current through this resistor being controlled by the CF Braking Chopper.

The rest of the paper is organized as follows: Section II describe the choice of DC link capacitor. In section III, the main parameters of leading inverter are defined and his section deals with the choice of IGBT modules. It is followed by the IGBT modules verification in Section IV. Section V and VI are related to the choice of the cooling system and the power cables. Finally, some concluding remarks are drawn.

## II. THE CHOICE OF THE DC LINK CAPACITOR

The following relationships are used to calculate the characteristic data for the inverter that supplies MAS1 [7]:

- Rated power,

$$S_{NINV1} = \frac{P_{1NMAS1}}{\cos \varphi_{MAS1} \eta_{MAS1}} = 188.6 \text{ kVA}, \quad (1)$$

where  $P_{MAS1}$ ,  $\cos \varphi_{MAS1}$ ,  $\eta_{MAS1}$  are the active power, the power factor and respectively the efficiency of machine MAS1.

As can be seen in the block diagram (Fig.1), the direct current intermediate circuit of the inverter INV1 is common with those of the inverter INV2, braking chopper CF and the filter of rectifier R and therefore the total capacitance value in the diagram was taken into account for the calculation of the capacitor bank.

To determine the required capacitance value we will consider the following conditions:

- ripple voltage allowed,

$$U_{RR} = 15\% \cdot U_{CC}; \quad (2)$$

For rated voltage  $U_{CC} = 750\text{V}$ , it results  $U_{RR} = 112.5\text{V}$ .

- the inverter efficiency,

$$\eta_{INV1} = 93\%;$$

- The input power of the inverter INV1,

$$P_{INV1} = S_{INV1} + p_{INV1} = 202 \text{ kW}, \quad (3)$$

where  $S_{INV1}$ ,  $p_{INV1}$  are the rated power and power losses of the inverter.

To calculate the needed capacitance, it can be used the following approached equation [8]:

$$C_{total} = \frac{P_{INV1}}{U_{RR} \left( U_{CC} - \frac{U_{RR}}{2} \right) f_R} = 8600 \mu\text{F}, \quad (4)$$

where:  $f_R$  - the rectifier frequency,  $f_R = 300\text{Hz}$ .

The RMS current through capacitor will be (approached equation) [8]:

$$I_{CRMS} = \frac{U_{RR}}{2\sqrt{2}} \cdot C_{total} \cdot 2 \cdot \pi \cdot f_R = 646 \text{ A}. \quad (5)$$

The needed capacitance for the inverter INV1:

$$C_{INV1} = C_{total} - (C_{INV2} + C_{CF} + C_R), \quad (6)$$

where:

$C_{INV2} = 4380 \mu\text{F}$  - capacitance value of the inverter INV2;

$C_{CF} = 1460 \mu\text{F}$  - capacitance value of the braking chopper CF;

$C_R = 1460 \mu\text{F}$  - capacitance value of the rectifier R.

We obtain  $C_{INV1} = 1300 \mu\text{F}$ .

Two ZEZ SILKO PVAJP 0 1,8/700 capacitors conected in parallel were selected with the main characteristics:

- rated capacitance  $C_N = 700 \mu\text{F} \pm 10\%$ ;
- rated DC voltage  $U_N = 1800\text{V}$ ;
- insulation voltage  $U_i = 4800\text{V}$ ;
- maximum rms current  $I_{max} = 150\text{A}$ ;
- operating temperatures  $\Theta_a = -25/+70\text{ }^\circ\text{C}$ .

The selection criteria are met as follows:

$$C_i \geq C_{icalc}; \quad (7)$$

$$U_N > U_{CCmax}; \quad (8)$$

$$I_{CRMS} \geq I_{CRMScalc}. \quad (9)$$

The inequality (9) results from the fact that all the capacitors in the common DC intermediate circuit are connected in parallel (8 capacitors that have the value  $I_{max} \geq 150\text{A}$ ), the value of the total current they can supply will add up, exceeding the value resulting from the calculations.

## I. THE CHOISE OF THE IGBT MODULE

The inverter output voltage is equal with the rated voltage of the electric machine [6].

$$U_{NINV1} = U_{NMAS1} = 500 \text{ V}_{AC}. \quad (10)$$

- The rated current phase of the inverter

Since the windings of the MAS1 electric machine are connected in star, the following results:

$$I_{NMAS1} = \frac{S_{NINV1}}{\sqrt{3} \cdot U_{NMAS1}} = 218 \text{ A}, \quad (11)$$

where:  $U_{NMAS1}$  – rated voltage of MAS1.

- Inverter overload power:

$$S_{SINV1} = 1.5 \cdot S_{NINV1} = 283 \text{ kVA}; \quad (12)$$

- Inverter overload phase current:

$$I_{SMAS1} = 1.5 \cdot I_{NINV1} = 327 \text{ A}; \quad (13)$$

- Inverter supply voltage range:

$$U_{CC} = 600 \div 900 \text{ V}_{CC}. \quad (14)$$

The power transistor shall be chosen with respect to the following relationships:

$$I_{TAVN} \cdot k_{SI} \leq I_{CCat}; \quad (15)$$

$$U_b \cdot k_{SU} \leq U_{CEScat}; \quad (16)$$

$$U_b = U_{cc}; \quad (17)$$

$$I_{TAVN} = \frac{\sqrt{2}}{\pi} \cdot I_{SMAS1} = 147.2 \text{ A}; \quad (18)$$

where:

$I_{TAVN}$  - the average rated current through the transistor;

- $I_{cat}$  - the maximum permissible average current through the transistor;
- $k_{si}$  - the current safety factor;
- $U_b$  - the voltage that stresses the transistor in off state;
- $U_{CES\ cat}$  - the maximum permissible voltage that stresses the transistor in off state;
- $k_{su}$  - the voltage safety coefficient;
- $U_{CC}$  - the intermediate circuit voltage.

Because the inverter is part of a research test bench where control errors may occur or higher power motors can be tested, the coefficients  $k_{su} = 1.8$ , respectively  $k_{si} = 10$  were chosen resulting:

$$U_{CES\ cat} > 1500\text{ V}; \quad (19)$$

$$I_{cat} > 1500\text{ A}. \quad (20)$$

The Mitsubishi **CM2400HC - 34H IGBT** module is preliminarily selected, with the main characteristics:

- capsule with a single IGBT - diode switching device;
- collector emitter voltage -  $V_{CES} = 1700\text{ V}$ ;
- direct collector current  $I_C = 2400\text{A}$ ;
- module dimensions :  $190 \times 140\text{ mm}$ .

An extract from the technical specification of this module is shown in Fig. 2. (a) and (b) [9].

### III. TESTING OF THE IGBT MODULE

Testing was done based on the **MELCOSIM Ver 5.4.0** application, developed by Mitsubishi for the selection of its own IGBT modules, arranged in the most common topologies.

MELCOSIM is designed for the calculation of the stationary and dynamic power losses that occur in modules as well as the temperature variation in the junctions of IGBT transistors and diodes in modules, due to both the direct conduction and switching of these semiconductor devices.

The corresponding data obtained for the specific dynamic thermal resistance of the power modules are used for the design, calculation and dimensioning of the heat sink.

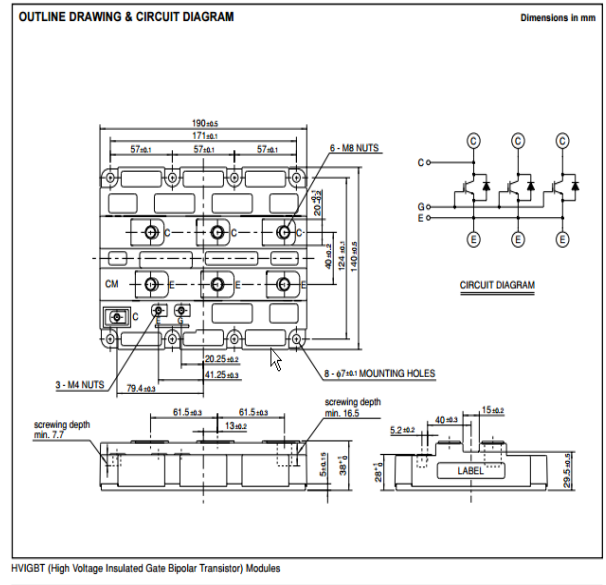
#### A. MELCOSIM Program Description

The converter type (two or three levels) can be selected from the main screen and then, switching in the screens for input and output data is done. The input-output screens consist of four sections: the module code and type, the specified module property, the input field "Common Conditions" for the converter characteristic data and the output field for the calculation results.

MELCOSIM expects nine entries called "Common Conditions" to be able to calculate power losses and temperature in the junction: modulation strategy, output current  $I_o$ , DC link  $V_{cc}$  voltage, switching frequency  $F_c$ , output frequency  $F_o$ , modulation factor  $M$ , load power factor  $PF_s$  and the heat sink temperature measured directly below the  $T_s$  capsule.

The results field provides the following information: average power losses for IGBT and freewheel diode, divided into static and dynamic parts, total power loss of the module, heat sink temperature, average and maximum temperature in the transistor junction and in the freewheel diode. The graphics output provides the possibility to

analyze power losses and temperature in junction by changing one of the application conditions parameters within the specification.



(a)

### CM2400HC-34H

HIGH POWER SWITCHING USE  
INSULATED TYPE

3rd-Version HVIGBT (High Voltage Insulated Gate Bipolar Transistor) Modules

#### MAXIMUM RATINGS

Symbol	Item	Conditions	Rated	Unit
$V_{CES}$	Collector-emitter voltage	$V_{GE} = 0V, T_j = 25^\circ C$	1700	V
$V_{GES}$	Gate-emitter voltage	$V_{CE} = 0V, T_j = 25^\circ C$	$\pm 20$	V
$I_C$	Collector current	$T_C = 80^\circ C$	2400	A
$I_{CM}$	Collector current	Pulse (Note 1)	4800	A
$I_E$ (Note 2)	Emitter current		2400	A
$I_{EM}$ (Note 2)	Emitter current	Pulse (Note 1)	4800	A
$P_C$ (Note 3)	Maximum power dissipation	$T_C = 25^\circ C$ , IGBT part	17800	W
$T_j$	Junction temperature		-40 - +150	$^\circ C$
$T_{op}$	Operating temperature		-40 - +125	$^\circ C$
$T_{stg}$	Storage temperature		-40 - +125	$^\circ C$
$V_{iso}$	Isolation voltage	RMS, sinusoidal, $f = 60\text{Hz}, t = 1\text{min}$ .	4000	V
$t_{psc}$	Maximum short circuit pulse width	$V_{CC} = 1150V, V_{CES} \leq 1700V, V_{GE} = 15V, T_j = 125^\circ C$	10	$\mu s$

#### ELECTRICAL CHARACTERISTICS

Symbol	Item	Conditions	Limits			Unit
			Min	Typ	Max	
$I_{CES}$	Collector cut-off current	$V_{CE} = V_{CES}, V_{GE} = 0V, T_j = 25^\circ C$	—	—	36	mA
$V_{GE(th)}$	Gate-emitter threshold voltage	$I_C = 240mA, V_{CE} = 10V, T_j = 25^\circ C$	4.5	5.5	6.5	V
$I_{GES}$	Gate leakage current	$V_{GE} = V_{GES}, V_{CE} = 0V, T_j = 25^\circ C$	—	—	0.5	$\mu A$
$V_{CE(sat)}$	Collector-emitter saturation voltage	$I_C = 2400A, V_{GE} = 15V, T_j = 25^\circ C$ (Note 4)	—	2.60	3.30	V
		$I_C = 2400A, V_{GE} = 15V, T_j = 125^\circ C$ (Note 4)	—	3.10	—	V
$C_{ies}$	Input capacitance	$V_{CE} = 10V, f = 100kHz$	—	210	—	nF
$C_{oes}$	Output capacitance	$V_{GE} = 0V, T_j = 25^\circ C$	—	30.0	—	nF
$C_{res}$	Reverse transfer capacitance	$V_{GE} = 0V, T_j = 25^\circ C$	—	10.1	—	nF
$Q_g$	Total gate charge	$V_{CC} = 850V, I_C = 2400A, V_{GE} = 15V, T_j = 25^\circ C$	—	19.8	—	$\mu C$
$V_{EC(max)}$	Emitter-collector voltage	$I_E = 2400A, V_{GE} = 0V, T_j = 25^\circ C$ (Note 4)	—	2.30	3.00	V
		$I_E = 2400A, V_{GE} = 0V, T_j = 125^\circ C$ (Note 4)	—	1.85	—	V
$t_{don}$	Turn-on delay time	$V_{CC} = 850V, I_C = 2400A, V_{GE} = \pm 15V$	—	—	1.60	$\mu s$
$t_r$	Turn-on rise time	$R_{G(on)} = 0.27\Omega, T_j = 125^\circ C, L_s = 80nH$	—	—	1.30	$\mu s$
$E_{on}$	Turn-on switching energy	Inductive load	—	810	—	mJ/pulse
$t_{d(off)}$	Turn-off delay time	$V_{CC} = 850V, I_C = 2400A, V_{GE} = \pm 15V$	—	—	2.70	$\mu s$
$t_f$	Turn-off fall time	$R_{G(off)} = 0.27\Omega, T_j = 125^\circ C, L_s = 80nH$	—	—	0.80	$\mu s$
$E_{off}$	Turn-off switching energy	Inductive load	—	870	—	mJ/pulse
$t_r$ (Note 2)	Reverse recovery time	$V_{CC} = 850V, I_C = 2400A, V_{GE} = \pm 15V$	—	—	2.70	$\mu s$
$Q_r$ (Note 2)	Reverse recovery charge	$R_{G(off)} = 0.27\Omega, T_j = 125^\circ C, L_s = 80nH$	—	—	630	$\mu C$
$E_{rec(max)}$ (Note 2)	Reverse recovery energy	Inductive load	—	—	330	mJ/pulse

Note 1. Pulse width and repetition rate should be such that junction temperature ( $T_j$ ) does not exceed  $T_{jmax}$  rating ( $125^\circ C$ ).  
 Note 2. The symbols represent characteristics of the anti-parallel, emitter to collector free-wheel diode (FWD).  
 Note 3. Junction temperature ( $T_j$ ) should not exceed  $T_{jmax}$  rating ( $150^\circ C$ ).  
 Note 4. Pulse width and repetition rate should be such as to cause negligible temperature rise.

(b)

Fig. 2 Extract from the technical specification of the IGBT module CM2400HC-34H.

All calculation results can be exported to a text file [10].

**B. IGBT Module Testing in Overload Conditions**

Testing the IGBT module in overload conditions was performed using the MELCOSIM application with the following input data (Fig 3):

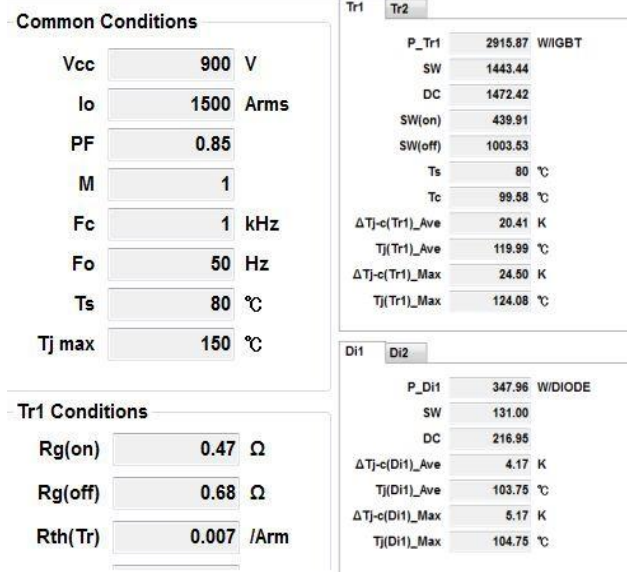


Fig. 3 „Common Condition” and „Result” fields for overload testing.

$V_{cc}$  - the maximum value for the DC circuit voltage, equal to the voltage that stresses the transistor in off state, respectively equal to the voltage limited by the braking chopper (CF) that is set to the value of 900 Vdc;

$I_o$  - The maximum output current of the asynchronous machine adjusted until the program no longer returns invalid messages.

The valid returned parameters correspond to the most unfavorable situation in which the device can operate for the chosen conditions, resulting:

$$I_o \gg I_{SMAS1} \quad (21)$$

**C. IGBT Module Testing for Operation in Rated Conditions (Fig 4):**

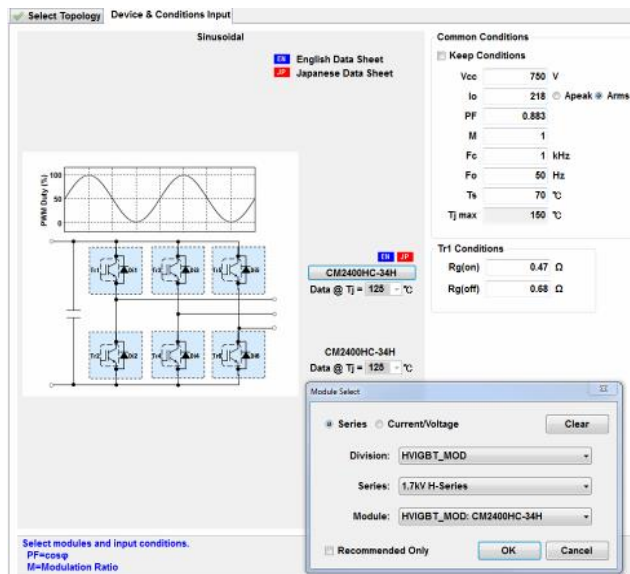


Fig. 4 The „Device & Components” screen for IGBT module testing at the rated condition operation.

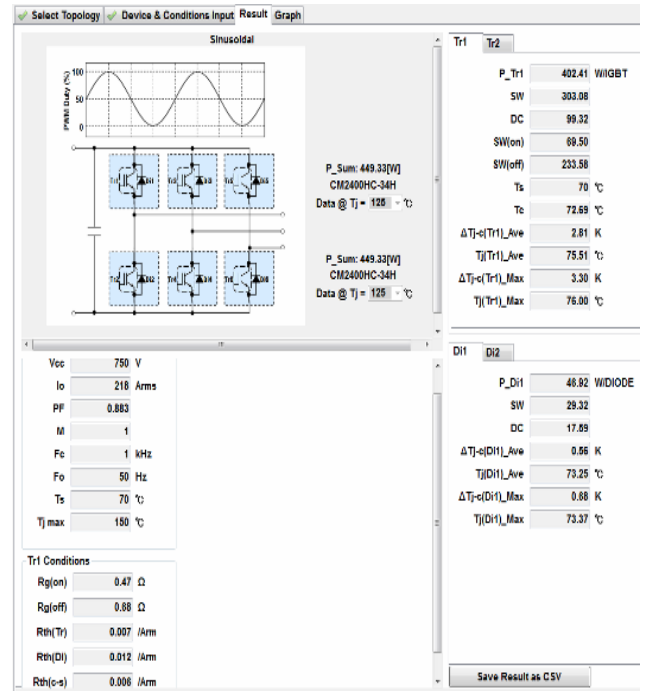


Fig. 5 "Result" screen with the characteristic values for the semiconductor components corresponding to a phase of the inverter.

The following parameters for the operation at rated load values have been introduced (Fig. 4 and Fig. 5):

- Input voltage  $V_{cc}$  ( $U_{ININV1}$ ) = 750 V ;
- Output rated current  $I_o$  ( $I_{NMA S1}$ ) = 218  $A_{RMS}$ ;
- Machine power factor  $PF$  ( $\cos\phi_{NMA S1}$ ) = 0.883;
- Modulation factor  $M$  = 1;
- Switching frequency  $F_c$  = 1 kHz;
- Converter output frequency  $F_o$  = 50 Hz;
- Heat sink temperature  $T_s$  = 70 °C.

The following considerations were considered in order to choose the gate control resistances which are relevant for the turn on and for the turn off process of the IGBT transistors, respectively:

- achieving minimal switching losses in both turn on and turn off by choosing the lowest possible resistance values;
- the peak current of the gate control devices.

The following values have been chosen using the data sheets:

- conduction input resistance  $R_{g(ON)} = 0.47 \Omega/1W$ ;
- blocking resistance  $R_{g(Off)} = 0.68 \Omega/1W$ .

**IV. CHOOSING THE COOLING SYSTEM**

The heat transfer diagram (Fig. 6) can be drawn up with the values obtained in the "Result" screen [11].

The "Graph" screen can generate the dissipated power versus time characteristic for two modules belonging to the same phase, giving additional information when multiple capsules are mounted on the same heat sink (Fig. 7).

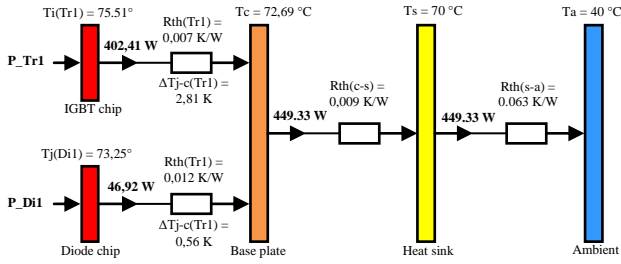


Fig. 6 The heat transfer diagram for the chosen IGBT module.

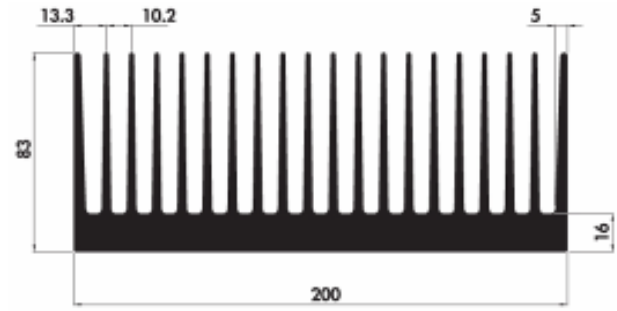


Fig. 8 Transversal section through the heat sink.

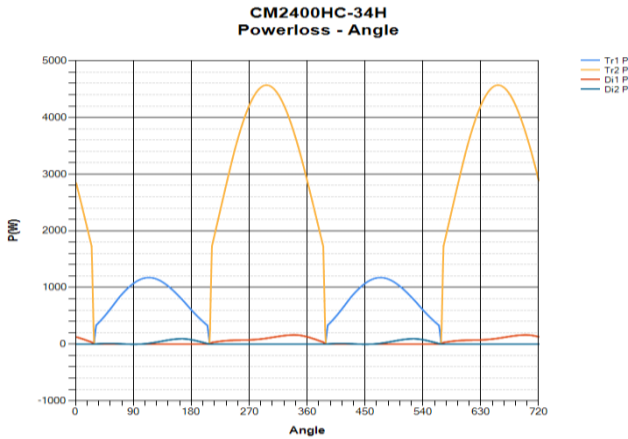


Fig. 7 Power dissipation versus time dependence for modules 1 and 2 of the inverters.

The heat transfer resistance between ambient and heat sink is:

$$Rth_{s-a} = \frac{T_c - T_a}{P_{Sum}} - Rth_{c-s} = 0.063 \text{ K/W}, \quad (22)$$

where:

- $T_c$  - case temperature;
- $T_a$  - ambient temperature;
- $P_{Sum}$  - total power dissipated by the module due to the conduction and commutation losses.

A heat sink is chosen from the catalog in order to meet the condition:

$$Rth_{s-cat} < Rth_{s-a,calc}, \quad (23)$$

where:

- $Rth_{s-a,calc}$  - calculated thermal resistance heat sink – ambient;
- $Rth_{s-cat}$  - thermal resistance heat sink – ambient catalog value.

A heat sink with the profile shown in Fig. 8 having a length of 250 mm, manufactured by MECCAL type P200 83 was chosen [12].

From the thermal transfer curves shown in Fig. 9, it can be seen that, provided an air speed of  $V_{air} = 7.2 \text{ m/s}$  through the heatsink with a length of 250 mm, the following resistance is obtained:

$$Rth_{s-a,cat} = 0.051 \text{ K/W}, \quad (24)$$

which is less than the value in (22), so the cooling system is chosen properly.

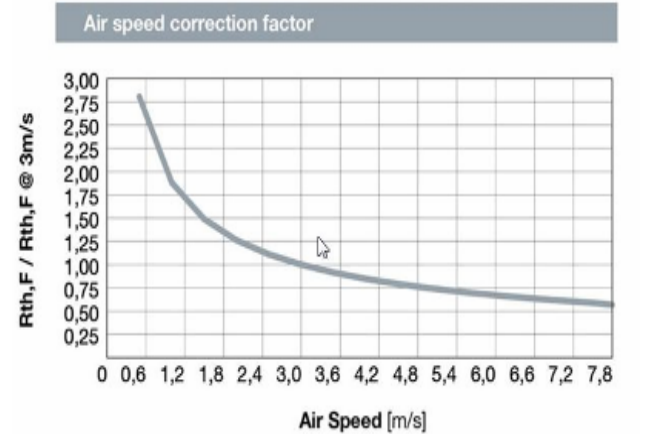
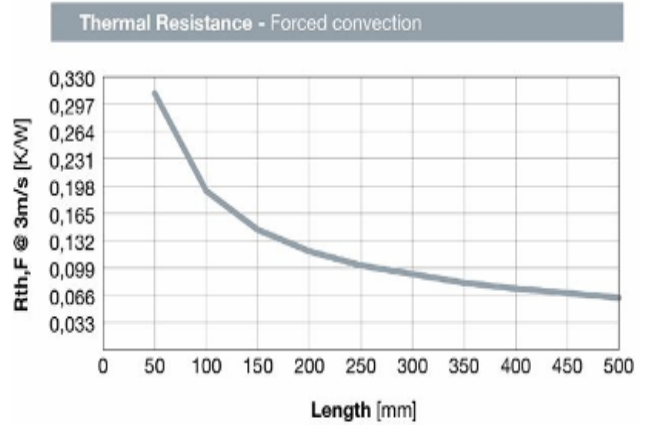


Fig. 9 The thermal transfer curves for the P200 83 heat sink.

## V. THE CHOICE OF THE POWER CABLES

The following characteristics of the inverters must be taken into account when dimensioning the cables:

- application: railway inverters;
- input voltage: 900 Vdc;
- rated current: 218 A;
- overload current: 327 A.

The cables used for railway rolling stock comply with the standard SR EN 50355:2014 “Railway applications - Railway rolling stock cables having special fire performance - Guide to use” [13].

The size of the cable section must be chosen from the standardized cable sections. When choosing the conductor section, the following factors will be taken into account:

- Electrical stresses in insulation, which are due to the operating voltage;

- Electrical stresses due to the intensity of the current flowing through the circuit and which must be lower than those allowed;
- Thermal stresses of the cables due to long-term, overload or short-circuit currents, taking into account the values indicated by the manufacturer and the application of the correction coefficients due to the positioning of the cables during installation as well as the maximum ambient operating temperatures.
- for cables up to  $1 \text{ mm}^2 U_0/U 300/500 \text{ V}$ ;
- for cables from  $1.5 \text{ mm}^2 U_0/U 450/750 \text{ V}$ ;
- at fixed and protected installation from  $1.5 \text{ mm}^2 U_0/U 600/1000 \text{ V}$ .
- Electrical stresses due to current intensity in the case of outdoor positioning:
  - for outdoor wiring situation  $70 \text{ mm}^2$  cable supports a current of 391 A, bigger than overload current – 327A.

Cables with the following codes were chosen:

- 51476 -  $70 \text{ mm}^2$  black cable;
- 51340 -  $2.5 \text{ mm}^2$  red cable;
- 51338 -  $2.5 \text{ mm}^2$  blue cable;
- 51298 -  $0.75 \text{ mm}^2$  red cable isolated in SCSI tube;
- 51296 -  $0.75 \text{ mm}^2$  blue cable isolated in SCSI tube.

The range of HELUTHERM 145 cables produced by HELUKABEL meets the required conditions [14].

Fig. 10 shows the catalog sheet for this type of cables and in Fig. 11 is figured the table of allowed currents and correction coefficients.

According to the catalog sheet, the selection criteria are met as follows:

- Electrical stresses in insulation, which are due to the operating voltage:

**Single Conductors**  
**HELUTHERM® 145** flexible, cross-linked, halogen-free ERC

**FRNC**  
**RoHS**

**Technical data**

- Halogen-free single cores with increased heat resistance
- **Temperature range**  
flexing  $-35^\circ\text{C}$  to  $+120^\circ\text{C}$   
fixed installation  $-55^\circ\text{C}$  to  $+145^\circ\text{C}$
- **Nominal voltage**  
up to  $1 \text{ mm}^2 = U_0/U 300/500 \text{ V}$   
from  $1.5 \text{ mm}^2 = U_0/U 450/750 \text{ V}$   
at fixed and protected installation from  $1.5 \text{ mm}^2 = U_0/U 600/1000 \text{ V}$
- **Test voltage** 3500 V
- **Minimum bending radius**  
flexing  $17.5 \times \text{core } \varnothing$   
fixed installation  $4 \times \text{core } \varnothing$
- **Caloric load values**  
see Technical Informations
- **Approval**  
Germanischer Lloyd

**Cable structure**

- Tinned copper conductor, to DIN VDE 0295 r1.5, line-wire, B5 6360 cl.5, IEC 60228 cl.5
- Core insulation of polyolefin-copolymer cross-linked and halogen free
- Core identification see table below

**Tests**

- Flame test (unit flame test) acc. to DIN VDE 0482-332-3-22, BS 4066 Teil 3, DIN EN 60332-3-22, IEC 60332-3-22 (previously DIN VDE 0472 part 804 test method C)
- Flame test (cable) acc. to DIN VDE 0482-332-1-2, DIN EN 60332-1-2, IEC 60332-1-2 (equivalent DIN VDE 0472 part 804 test method B)
- Corrosiveness of combustion gases acc. to DIN VDE 0482 part 267, DIN EN 50267-2-1, IEC 60754-1 (equivalent DIN VDE 0472 part 815)
- Smoke density acc. to DIN VDE 0482 part 1034-1+2, DIN EN 61034-1+2, IEC 61034-1+2, BS 7622 part 1+2 (previously DIN VDE 0472 part 816)

**Properties**

- Lower propagation of fire
- Low development of smoke and fumes
- Good abrasion and notch resistance
- Good resistance to oils and weathering
- Resistant to UV radiation and ozone
- Resistant to soldering temperatures
- Thermal class B
- These single-core cables are resistant to melting, even when in contact with a soldering iron at temperatures of between  $300^\circ\text{C}$  and  $380^\circ\text{C}$ , because of the cross-linking for the insulation material
- Due to the high temperature profile the cross-section of conductor can under certain circumstances be reduced, hereby enabling a saving in space requirement and weight
- The materials used in manufacture are cadmium-free and contain no silicone and free from substances harmful to the wetting properties of lacquers.

**Application**

These temperature resistant single-core cables are used for the internal wiring of lighting fixtures, heaters, electrical machinery, switching systems and distributors in equipment and plant and machinery, suitable for laying in tubes on and under plaster, in closed installation ducts, as well as for traffic systems and outdoor applications. These cables are not approved for direct routing on racks, gutters or tanks. For a protected installation, these cables may be used at a nominal voltage of up to 1000 V alternating current or a direct current up to 750 V when earthed. The maximum operating d. c. voltage used in rail vehicles shall not exceed 900 V when earthed. These halogen-free single-core cables are characterised by their amazingly high long-time resistance to temperature and feature among the leading halogen-free, flame resistant products in the world. These single-core cables significantly contribute to safety and the environment.

**CE** – The product is conformed with the EC Low-Voltage Directive 2006/95/EC.

Cross-section, mm <sup>2</sup>	Outer Ø approx. mm	Cop. weight approx. kg/km	Weight approx. kg/km	DK	DN-YE	BL	BN	RD	WH	GY	VT	YE	GN	D-BU	OG	BEIGE	3-col.
0.25	1.8	2.4	4.3	5044	5048	5107	5107	5107	5107	5107	5107	5107	5107	5107	5107	5107	5115
0.35	2.1	3.2	5.9	5117	5116	5118	5118	5118	5117	5117	5117	5117	5117	5117	5117	5117	5119
0.5	2.4	4.8	7.0	5121	5120	5122	5122	5122	5121	5121	5121	5121	5121	5121	5121	5121	5123
0.75	2.7	7.2	11.0	5125	5124	5126	5126	5126	5125	5125	5125	5125	5125	5125	5125	5125	5127
1	3.0	9.6	14.0	5129	5128	5130	5130	5130	5129	5129	5129	5129	5129	5129	5129	5129	5131
1.5	3.6	14.4	20.9	5133	5132	5134	5134	5134	5133	5133	5133	5133	5133	5133	5133	5133	5135
2.5	4.5	24.0	39.0	5137	5136	5138	5138	5138	5137	5137	5137	5137	5137	5137	5137	5137	5139
4	6.3	38.0	67.0	5141	5140	5142	5142	5142	5141	5141	5141	5141	5141	5141	5141	5141	5143
6	8.1	58.0	102.0	5145	5144	5146	5146	5146	5145	5145	5145	5145	5145	5145	5145	5145	5147
10	11.0	96.0	170.0	5149	5148	5150	5150	5150	5149	5149	5149	5149	5149	5149	5149	5149	5151

Fig. 10 HELUTHERM 145 cable catalog sheet.

**CURRENT RATINGS FOR HELUTHERM® 145**  
 Operating temperature at conductor 120° C

For permanent operating to the ambient temperature of 30° C. Conversion factors for the deviating site operation conditions – see tables below.  
 Sufficiently large or ventilated rooms in which the ambient temperature is not noticeably increased by the heat losses from the cables. Protection should be taken from the solar radiation etc.

Installation				
Conversion factors for grouping	–	to table 1	to table 2	to table 3
Current ratings in Ampere (A) up to 30°C ambient temperature				
Cross-section, mm <sup>2</sup>				
0,25	13	12	9	7
0,33	17	15	11	9
0,50	19	18	12	10
0,75	24	23	17	13
1,0	31	30	20	17
1,5	39	36	25	20
2,5	51	48	33	26
4	68	65	45	36
6	88	84	58	46
10	121	116	80	64
16	160	152	106	85
25	211	200	140	111
35	261	248	172	138
50	370	354	241	199
70	411	391	272	217
95	502	476	331	265
120	587	558	387	310
150	680	646	449	359
185	781	743	516	413
240	931	884	614	492

Number of single core cables for 2 phase or 3 phase systems	1	2	3	4	5	6	7	8	9	10	12
Table 1	Factor	1,00	0,94	0,90	0,90	0,90	0,90	0,90	0,90	0,90	0,90
Table 2	Factor	1,00	0,85	0,79	0,75	0,73	0,72	0,72	0,71	0,70	–
Table 3	Factor	1,00	0,80	0,70	0,65	0,60	0,57	0,54	0,52	0,50	0,48

Temperature in °C	20	30	40	50	60	70	80	90	95	100	105	110	115
Factor	1,05	1,00	0,94	0,88	0,82	0,75	0,67	0,58	0,53	0,47	0,41	0,33	0,24



10/3

Fig. 11 Current ratings for HELETHERM 145.

**VI. CONCLUSIONS**

The research conducted in this paper highlights the fact that when choosing the force components for a test – experimentation bench designed to test various control strategies for traction converters, it is necessary to consider the addition of bigger safety coefficients than usual at their technical characteristics covering some control errors which may occur. It has also been shown that a forced ventilation cooling system is suitable, cheaper and less complex than a liquid cooling one.

**ACKNOWLEDGMENT**

This work was supported by the grant POCU380/6/13/123990, co-financed by the European Social Fund within the Sectorial Operational Program Human Capital 2014 – 2020.

**Source of research funding in this article:** grant POCU380/6/13/123990.

Contribution of authors:

First author – 50%

First coauthor – 30%

Second coauthor – 20%

Received on August 10,2021

Editorial Approval on November 30, 2021

**REFERENCES**

- [1] X. Huang, W. Chang and T. Q. Zheng, “Study of the protection and driving characteristics for high voltage high power IGBT modules used in traction convertor,” 2015 IEEE 10th Conference on Industrial Electronics and Applications (ICIEA), Auckland, New Zealand, 2015, pp. 1330-1334.
- [2] M. M. Bakran, H. Eckel, M. Helsper and A. Nagel, “Next Generation of IGBT-Modules Applied to High Power Traction,” 2007 European Conference on Power Electronics and Applications, Aalborg, Denmark, 2007, pp. 1-9.
- [3] K. Sheng, B.W. Williams, X. He, Z. Qian, S.J. Finney, “Measurement of IGBT switching frequency limits,” Power Electronics Specialists Conference, 1999, PESC 99. 30<sup>th</sup> Annual IEEE.
- [4] S. C. Das, A. Tiwari, G. Narayanan and A. K. Kumar, “Experimental investigation on switching characteristics of IGBTs for traction application,” 2012 IEEE International Conference on Power Electronics, Drives and Energy Systems (PEDES), Bengaluru, India, 2012, pp. 1-5.
- [5] M. B. Inarra, I.B. Zubiaurre, I.L.Bengoetxea, I.Z. Azaceta, “Power Electronic converter. Design Book”.
- [6] L. S. Goreci, M. Popescu and I. Tilă, "The choice of the IGBTs and their cooling in electric traction converters for autonomous vehicles," 2021 International Conference on Applied and Theoretical Electricity (ICATE), Craiova, Romania, 2021, pp. 1-5.
- [7] M. Popescu, A. Bitoleanu, D. Mihai, C. Constantinescu, "Convertoare statice si structuri de comandă performante", Editura Sitech,2000.
- [8] AVX: Medium Power Film Capacitors, Application Notes
- [9] Mitsubishi HVIGBT Modules CM2400HC-34H, [https://www.mitsubishielectric-mesh.com/products/pdf/cm2400hc-34h\\_e.pdf](https://www.mitsubishielectric-mesh.com/products/pdf/cm2400hc-34h_e.pdf).
- [10] Simulation soft, Mitsubishi Electric Power Module Loss Simulator, [http://sem.mitsubishielectric.eu/products/power\\_semiconductors/melcosim](http://sem.mitsubishielectric.eu/products/power_semiconductors/melcosim)
- [11] R. Künzi, “Thermal design of power electronic circuits,” CERN Yellow Report CERN-2015-003, pp.311-327.
- [12] Air cooled technologies. Heat sinks catalogue, <http://www.meccal.com/en/download/catalogo-prodotti-aria.pdf>.
- [13] SR EN 50355:2014 “Railway applications - Railway rolling stock cables having special fire performance - Guide to use”
- [14] Helutherm 145 Cable <https://helukabel-sea.com/wp-content/uploads/2018/07/HELUTHERM%C2%AE-145.pdf>